Journal of Solid State Chemistry 184 (2011) 1236–1244

Contents lists available at ScienceDirect

Journal of Solid State Chemistry

journal homepage: www.elsevier.com/locate/jssc

Study of carbon dioxide adsorption on a Cu-nitroprusside polymorph

R. Roque-Malherbe [a,*], C. Lozano [a], R. Polanco [a], F. Marquez [a], F. Lugo [a], A. Hernandez-Maldonado [b], J.N. Primera-Pedrozo [b]

[a] Institute for Physical Chemical Applied Research, School of Science, University of Turabo, P.O. Box 3030, Gurabo, PR 00778-3030, USA
[b] Department of Chemical Engineering, University of Puerto Rico-Mayagüez Campus, Mayagüez, PR 00681-9000, USA

ARTICLE INFO

Article history:
Received 30 November 2010
Received in revised form
2 February 2011
Accepted 27 February 2011
Available online 13 April 2011

Keywords:
Adsorption space
Cu-nitroprusside
Molecular interaction
Confinement
Lewis acid

ABSTRACT

A careful structural characterization was carried out to unequivocally determine the structure of the synthesized material. The TGA, DRIFTS and a Pawley fitting of the XRD powder profiles indicate that the hydrated and *in situ* dehydrated polymorph crystallizes in the orthorhombic space group *Pnma*. Meanwhile, the CO_2 isosteric heat of adsorption appears to be independent of loading with an average value of 30 kJ/mol. This translates to a physisorption type interaction, where the adsorption energy corresponding to wall and lateral interactions are mutually compensated to produce, an apparently, homogeneous adsorption energy. The somewhat high adsorption energy is probably due to the confinement of the CO_2 molecules in the nitroprusside pores. Statistical Physics and the Dubinin theory for pore volume filling allowed model the CO_2 equilibrium adsorption process in Cu-nitroprusside. A DRIFTS test for the adsorbed CO_2 displayed a peak at about 2338 cm^{-1} that was assigned to a contribution due to physical adsorption of the molecule. Another peak found at 2362 cm^{-1} evidenced that this molecule interacts with the Cu^{2+}, which appears to act as an electron accepting Lewis acid site. The aim of the present paper is to report a *Pnma* stable Cu-nitroprusside polymorph obtained by the precipitation method that can adsorb carbon dioxide.

1. Introduction

Transition metal cyanides (Prussian blue analogs [1–4] and nitroprussides [5–15]) display frameworks assembled with transition metals, bridged through the linear cyanide ion. This structure possesses interesting properties, such as, physical adsorption [4,13–15], light induced phenomena [3], magnetism [16] and other properties that make these materials an interesting class of porous coordination polymers.

Nitroprussides (pentacyanonitrosylferrates), are a group of metal cyanides, consisting of porous frameworks that are constructed from: $[Fe(CN)_5NO]^{2-}$, building units bridged though, M^{2+}, cations, by means of the CN^- ligands [5–15]. In this tridimensional framework the O, atom at the end of the, NO ligands, remains permanently free [5] and the, M^{2+}, cation normally coordinates to one or more water molecules while the rest of the water molecules are hydrogen bonded to the coordinated water molecules [6–8]. These at the same time are filling the adsorption space (pore volume) produced by the formation of the nitroprusside framework. Consequently, after thermal dehydration both the coordinated and the hydrogen-bonded or zeolitic water molecules are detached, leading to materials with a channel system suitable for the adsorption of small molecules [13–15]. Additionally, Mn, Fe, Co, Ni, and Cu nitroprusides, normally, follow the modified Curie–Weiss law, a characteristic behavior of paramagnetic materials, and at low temperatures shows ferromagnetic order [16].

Adsorption [17–20] is an important property of nitroprussides [13–15], which exhibit, additionally, magnetic properties [16]. This fact could bring the opportunity of changing the magnetic behavior by controlling the electronic structure of the nitroprusside through adsorbed molecules, and then produce novel sensors.

A very good probe to study adsorption on microporous materials is the carbon dioxide molecule [21–23]. Specifically, carbon dioxide adsorption data is an excellent tool for the measurement of the micropore volume [24,25] and adsorption interactions [26,27]. Additionally, a very useful tool for the study of the physical and chemical properties of solid surfaces is the infrared spectra of adsorbed carbon dioxide, since this molecule is a small and weakly interacting probe adsorbate [21–23].

The structure of Cu-nitroprusside (Cu-NP) has been studied for nearly two decades [8,9], but their polymorphic nature still requires more effort for complete understanding of the properties of these materials. Stable Cu-NP crystallizes, in the *Pnma* space group with a framework where Fe atoms are coordinated by five

* Corresponding author. Fax: +1 787 743 7979x4114.
E-mail addresses: RRoque@suagm.edu, RRoquemalh@aol.com (R. Roque-Malherbe).

0022-4596/$ - see front matter © 2011 Elsevier Inc. All rights reserved.
doi:10.1016/j.jssc.2011.02.029

CN ligands and a NO group and Cu atoms are coordinated by five CN and a H_2O molecule, and the second water molecule is H-bonded to the coordinated water [8]. In the case of the hydrated Cu-NP fresh precipitates, however, there are reported a mixture of two tetragonal phases [9] and a polymorph crystallizing in the space group *Amm2*, where Fe atoms are coordinated to five CN ligands and a NO group, while the Cu atoms are coordinated by four CN and two H_2O molecules [13]. Additionally, it has been reported that the dehydrated on heating *Amm2* Cu-nitroprusside phase experiences a transformation to, an anhydrous, tetragonal space group *I4mm* phase [15]. Subsequently, minor changes in the preparation process could lead to materials with fairly different properties, requiring this careful characterization to unambiguously identify the tested polymorph and this is one of the aims of the present paper.

Here we present the adsorption properties of a Cu-NP on a well characterized polymorph in order to carefully explore the volume of the available adsorption space, the intensity of the adsorption field and the specific interactions of the carbon dioxide molecule with the Cu-NP framework. To accomplish these objectives we have employed energy dispersive X-ray spectroscopy (EDAX), thermogravimetric analysis (TGA), X-ray diffraction (XRD), diffuse reflectance infrared Fourier transform spectrometry (DRIFTS) and volumetric adsorption of carbon dioxide at 273 and 298 K. The information obtained about the studied material will be employed to explore its application as a sensor to small molecules, adsorption and catalysis. Particularly, adsorption related applications of the Cu-NP polymorph studied here, has not been studied. Since, these materials include paramagnetic metal centers of the first row transition metals [28], we will emphasize in the effect of adsorption on magnetic properties.

2. Experimental section

2.1. Materials and synthetic procedure

All the consumed chemicals were analytical grade without additional purification. The water used in the synthesis process was bi-distilled.

The produced nitroprussides were synthesized by adding 0.025 moles of solid $Na_2[Fe(CN)_5NO]\cdot 2H_2O$ to a solution containing 0.025 moles of the corresponding copper(II) salt, that is, $Cu(NO_3)_2$ or $CuSO_4$, in 250 mL water under constant stirring. The formed precipitates were then separated, successively washed with distilled water and dried at 70 °C during 24 h. Accordingly, two samples were obtained, one synthesized with the $Cu(NO_3)_2$ solution and the other produced with the $CuSO_4$ solution. In both cases, the final concentrations of the reagents were 0.1 M. In previous reports 0.01 M solutions were normally used [15]; subsequently, in the present case relatively concentrated solutions were applied in order to get a material with different properties.

Both samples were studied applying EDAX, TGA, DRIFTS, XRD and adsorption of carbon dioxide. For both materials were obtained exactly the same results, consequently the use in the synthesis of $Cu(NO_3)_2$ or $Cu(SO_4)$ solutions has no influence on the obtained Cu-nitroprussides. Then, in the present paper were only reported the results related to the Cu-NP sample, synthesized with $Cu(NO_3)_2$ solution.

2.2. Characterization methods

Elemental chemical analysis on Cu-NP were performed using an energy dispersive X-ray (EDAX) spectrometer couple to a JEOL Model JSM-6360 scanning electron microscope (SEM), equipped with an energy dispersive X-ray analysis detector. The acceleration of the electron beam was 20 kV. The sample grains were glued with silver colloid to the sample holder and covered with palladium previous to the analysis. In order to guarantee, that we were testing a sample with a homogeneous distribution of Cu and Fe within the sample, were analyzed ten spots. A small dispersion of the concentration of Cu and Fe was demonstrated by the obtained results, warranting an acceptable homogeneity.

The TGA testing process was carried out with a TA, Q-500 instrument [18]. Samples were placed onto a ceramic sample holder suspended from an analytical balance. The sample and holder were heated according to a predetermined thermal cycle: the temperature was linearly scanned, from 25 to 300 °C, at a heating rate of 5 °C/min under a pure N_2 flow of 100 ml/min. The instrument software all automatically controlled data collection, temperature control, heating rate, and gas flow. The TGA data was collected as a $W_t\%$ versus T (°C) profile, where $W_t\% = (M_t/M_0)\times 100$ is the percent ratio of the sample mass during the thermal treatment, M_t, and the initial mass of the sample M_0.

Diffuse reflectance infrared Fourier transform spectra (DRIFTS) were gathered using a Thermo Scientific Nicolet iS10 FTIR spectrometer. The data of the hydrated and dehydrated samples were collected at a resolution of 4 cm^{-1} employing 100 scans per sample. A background, with pure KBr, provided by Nicolet, applying the same conditions was always gathered previous to sample collection. Both the hydrated and dehydrated samples spectra were obtained at room temperature under N_2 (Praxair, 99.99%) flowing at a rate of 50 cm^3/min. Before the analysis the dehydrated samples were previously treated at 100 °C, for 2 h under a N_2 flow applying the previously reported conditions. For gathering of the DRIFTS spectra for the Cu-NP with adsorbed carbon dioxide, the background was carefully measured using the dehydrated sample at room temperature. Afterwards, CO_2 (Praxair, 99.99%) was allowed into the sample chamber of the IR high temperature cell at flow at a rate of 50 cc/min rate for three minutes followed by purging under N_2 (Praxair, 99.99%) at the same flow rate for one minute. Spectra of the carbon dioxide molecule adsorbed on the Cu-NP framework were then obtained at room temperature under N_2 flow.

X-ray diffraction tests were carried out using a Bruker D8 Advance system in a Bragg-Brentano vertical goniometer configuration. The angular measurements were made with a (Theta/2Theta) of $\pm$0.0001 reproducibility, applying steps of 0.01° from 5° to 60° to get XRD profiles that could be accurately resolved by least square methods. The X-ray radiation source was a ceramic X-ray diffraction Cu anode tube type KFL C 2 K of 2.2 kW, with long fine focus. A variable computer-controlled motor driven divergence slit with 2.5°. Soller slit was included to allow to keep the irradiated area on the sample surface constant. A Ni filter was placed, prior to the detector, to eliminate Cu$K\beta$ radiation. A LynxEye™ one-dimensional detector was employed. This detector is based on a Bruker AXS compound silicon strip technology and increases measured intensities, without sacrificing resolution and peak shape. This together with the use of small scanning step resulted in high quality XRD profiles suitable for mathematical treatment. High temperature measurements in vacuum were performed using an Anton Paar HTK-1200N stage. This high-vacuum chamber was designed to be used in the range from room temperature up to 1200 °C. The sample was mounted on an alumina sample holder with temperature sensor located just below the sample.

Carbon dioxide equilibrium adsorption at 273 K and at pressures up to 1 atm was carried out in an upgraded Quantachrome Autosorb-1 automatic volumetric physisorption analyzer. The measurements at 298 K and pressures up to 7 atm were obtained with a Micromeritics ASAP 2050 static volumetric adsorption

system. The adsorption isotherms of CO_2 (Praxair, 99.99%) at 273 and 298 K were obtained for samples degassed at 373 K for 5 h in high vacuum (10^{-6} Torr). The backfilling process was carried out using helium (Praxair, 99.99%) in both cases.

3. Results and discussion

3.1. Structural characterization

Elemental chemical analysis of the nitroprusside samples were carried out with a SEM equipped with an energy dispersive X-ray analysis detector. The measurement yielded: Fe/Cu ≈ 1/1 in accordance with the formula unit of this nitroprusside, i.e. $Cu[Fe(CN)_5NO]\cdot xH_2O$. The water amount xH_2O was estimated using TGA measurements [7,8]. The thermal gravimetric profile is shown in Fig. 1, while the derivative of this profile is presented in Fig. 2. It is evident that at relatively low temperatures, that is, below 100 °C the water is released in two steps. This fact was confirmed in Fig. 2, where this shape was resolved in two peaks.

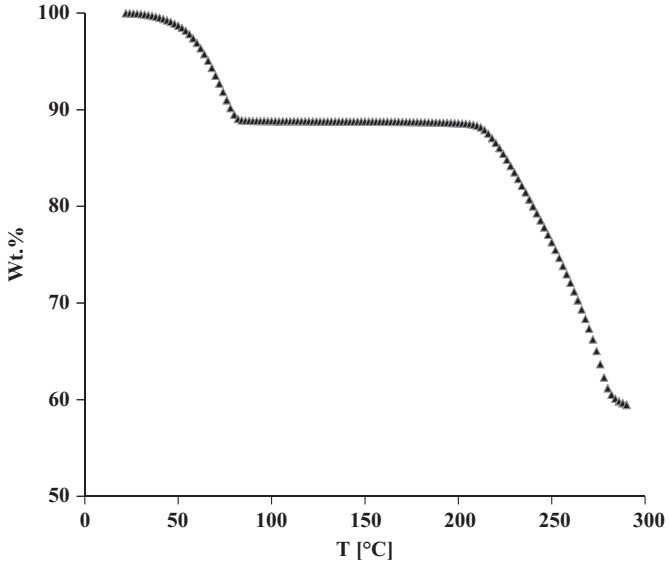

Fig. 1. TG profile of the Cu-NP sample.

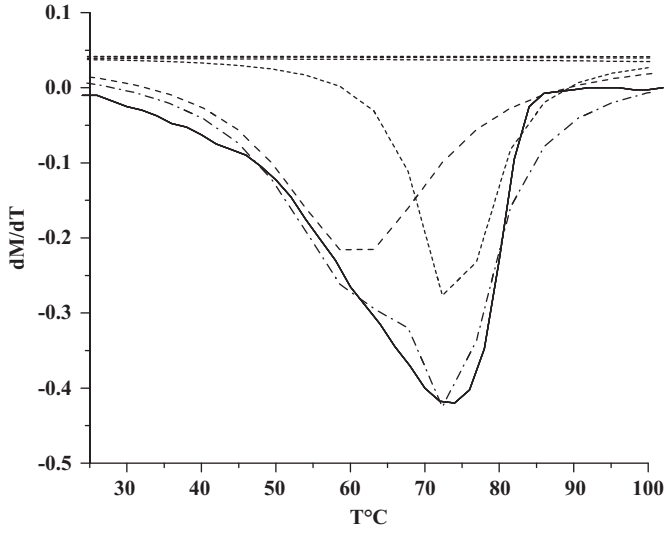

Fig. 2. Derivative of the TG profiles of the Cu-NP sample.

These peaks can be related, sequentially, to the liberation of hydrogen-bonded water and coordinated water, respectively.

The total weight lost during to water elimination corresponds to approximately 11 wt%, or about $2H_2O$ molecules per formula unit. Consequently, the formula unit of the tested Cu-NP should be $Cu[Fe(CN)_5NO]\cdot 2H_2O$ [8].

Meanwhile the obtained nitroprusside appears to be stable from 100 to 200 °C as evidenced by the absence of any appreciable changes in that region of the TGA profile. Finally, the weight lost observed after at 200 °C could be related to the decomposition of the nitroprusside by the liberation of the structural NO and CN groups contained in the framework [7]. It should be mentioned that the previously reported results are typical of the *Pnma* Cu-NP polymorph, which is the stable form of this nitroprusside [8] obtained by the slow diffusion tube methodology [6,7]. However, the polymorph tested here was obtained by the precipitation method. It is our assessment that was produced the stable *Pnma*, as a consequence of the addition of powdered solid $Na_2[Fe(CN)_5NO]\cdot 2H_2O$ to the corresponding copper(II) salt.

DRIFT spectra of the Cu-NP sample (hydrated and dehydrated) in the range between: 1400–2400 and 3200–3800 cm^{-1}, are shown in Fig. 3. IR data in the range between: 1400 and 2400 cm^{-1}, in inorganic compounds, contain information about the framework vibrations and those in the range 3200–3800 cm^{-1} include information related, essentially, with the hydration water [29].

Fig. 3 shows the vibrations observed in the range between: 1400 and 2400 cm^{-1}, which are related with the ν(CN) stretching vibration at around 1610 cm^{-1}, a 1950 cm^{-1} band corresponding to ν(NO)stretching vibration and a 2200 cm^{-1} band due to $\delta(Fe-C\equiv N)$ vibration [7,8,30–32]. All these vibrations are maintained after dehydration (Fig. 3) with only minor shifts, excluding the ν(CN) stretching vibration corresponding to the unlinked cyanide which disappears. It is necessary to state that this band possibly vanish because all the CN are linked in the dehydrated state [13]. Vibrations related to the water molecules contained in the nitroprusside are usually present in the 3200–3800 cm^{-1} range. In Fig. 3 these contributions are characterized by one broad at 3250–3400 cm^{-1} range and a narrow one at around 3650 cm^{-1}. It is a very well known fact that the hydrogen bonded water, shows a broad stretching, ν(OH), absorption bands approximately in the range between: 3250 and 3400 cm^{-1} [29]. On the other hand, the coordinated water exhibits a comparatively narrow band around 3650 cm^{-1} [30]. Both bands disappear after dehydration.

In general DRIFTS results correlate well with the TGA data. That is, IR absorption bands in the 3200–3800 cm^{-1} range are related to hydrogen-bonded water and coordinated water, respectively. Then, the IR profile in this range is also characteristic of the stable *Pnma* polymorph of Cu-NP [8]. For hydrated Cu-NP fresh precipitates as was previously stated, there are reports of at least two polymorphs [13]. The polymorphic nature of nitroprussides is associated to the way that CN and H_2O ligands are coordinated to the cation *M* [6–9]. In the case of the stable *Pnma* polymorph of Cu-NP, five cyanide groups and one water molecule are bonded to the Cu cation and the other water molecule is hydrogen-bonded to the coordinated water molecule [8]. The polymorph normally obtained from fresh precipitates, crystallizes in the *Amm*2 space group, where the Cu atoms are coordinated by four CN and two H_2O molecules [13]. This is not the case here and therefore we must suspect that our synthesized Cu-NP crystallizes in the orthorhombic *Pnma* space group. However, in order to substantiate this hypothesis we must consider a thorough XRD analysis.

Fig. 4 shows the XRD profile gathered for the hydrated Cu-NP sample in the range between 5° and 60° in 2θ. In order to resolve the powder XRD profile into separate Bragg components and in the absence of any concrete structural model was applied the

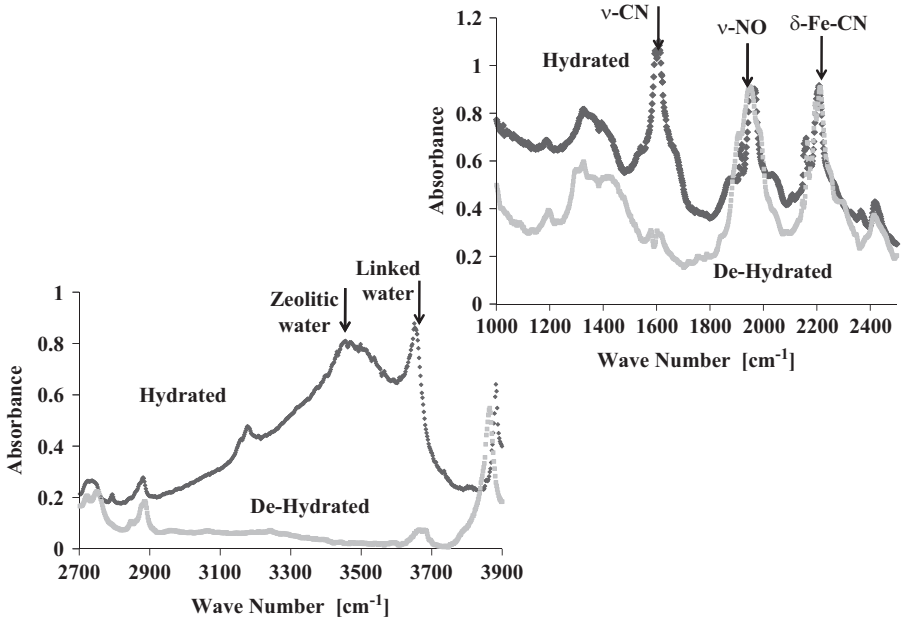

Fig. 3. DRIFTS spectra of sample hydrated and dehydrated Cu-NP sample.

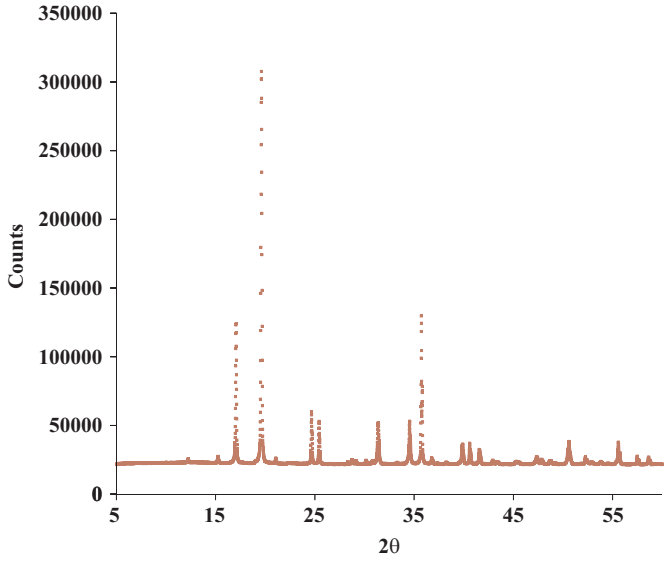

Fig. 4. XRD profiles of the hydrated Cu-NP sample.

pattern decomposition method [33]. More concretely was applied the Pawley whole-powder pattern decomposition (WPPD) method [34]. This method can refine the unit cell parameters and decompose the whole powder pattern into individual reflections [33]. The concrete computer program used to carry out the calculations was the Bruker DIFFRAC*plus* TOPAS™ software.

Fig. 5 shows the resulting fitting of the hydrated Cu-NP powder pattern for the orthorhombic *Amm*2 and *Pnma* space groups. Table 1 collects the cell parameters, the cell volume and the *R* factor. The obtained data (Table 1) show a good fitting for both the *Amm*2 polymorph [15] and *Pnma* stable polymorph [8]. However, a somewhat better fitting was obtained for the orthorhombic *Pnma* space group. This result together with TGA and DRIFTS data presented above allow us to reasonably propose that the tested Cu-NP crystallizes, in the hydrated state, in the orthorhombic *Pnma* space group with: $a=14.41534$ Å, $b=6.99627$ Å, $c=10.38027$ Å cell parameters.

As was previously stated, it has been reported that dehydrated *Amm*2 Cu-nitroprusside polymorph experiences a phase transformation to an anhydrous, tetragonal space group *I*4*mm* phase upon heating [15]. Fig. 6 shows the fittings of the XRD profile of the dehydrated Cu-NP sample at 100 °C for 2 h in vacuum and collected at room temperature also in vacuum inside the high temperature cell for the orthorhombic *I*4*mm* and *Pnma* space groups. Table 1 also shows the corresponding cell parameters, cell volume and *R* factor. The obtained results demonstrate a good fitting for the *I*4*mm* space group and an excellent fitting for the *Pnma* space group. That is, a better fitting was obtained for the orthorhombic *Pnma* space group. Thereafter, as a consequence of the better fitting of the refined XRD data; and the fact that the *Pnma* phase is the stable phase of Cu-NP, we propose that the polymorph studied here crystallized in the anhydrous state in an orthorhombic space group *Pnma* phase, with the following cell parameters: $a=14.83321$ Å, $b=12.2363$ Å, $c=9.89889$ Å. However, this assignment is some sense in contradiction with the disappearance of the ν-CN band corresponding to the unlinked CN; since, this fact is characteristic of the transition from the orthorhombic *Amm*2 phase to the *I*4*mm* tetragonal phase during dehydration [13]. In this regard, we can give an explanation to this fact by the enlargement of the parameter *b* of the orthorhombic dehydrated *Pnma* (Table 1), which indicates a phase transformation during dehydration to a cell similar to the tetragonal *I*4*mmm*.

3.2. Carbon dioxide adsorption study

The framework of the Cu-NP contains distorted octahedral metal centers that are linked by cyanide bridging in a staggered way creating micropores that pervades the crystal lattice [8]. This framework looks as a stack of rippled sheets connected by cyanide bonds and consequently we are dealing with a microporous crystalline adsorbent showing a 3-dimensional channel system [13], with pore diameters in the range of the carbon dioxide molecular diameter (carbon dioxide is a molecule with an ellipsoidal form 5.4 Å long and a diameter of 3.4 Å [35]).

We should expect adsorption of carbon dioxide molecules in the synthesized Cu-NP in the anhydrous state. To prove that the tested Cu-NP adsorbs carbon dioxide, Fig. 7a shows logarithmic in

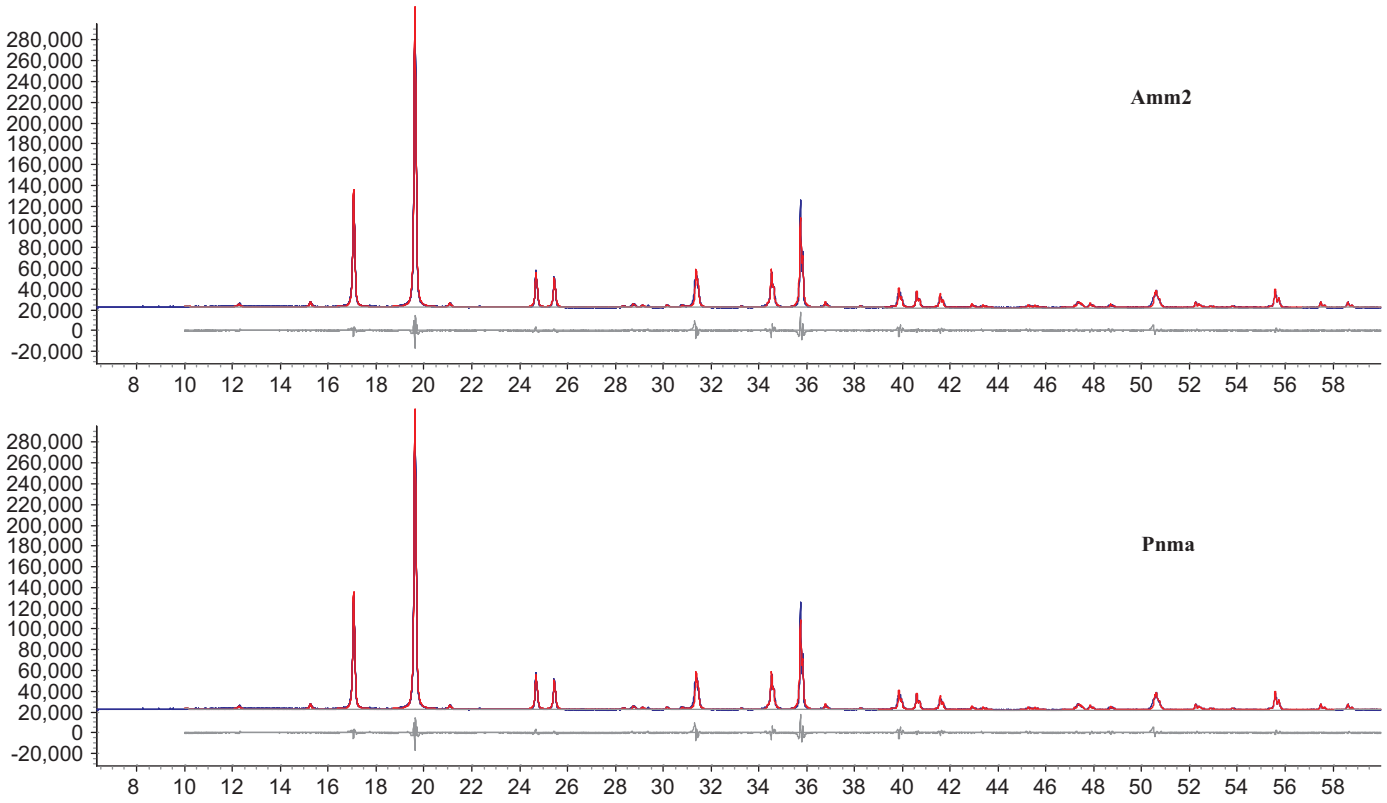

Fig. 5. Pawley refinement of the XRD of the hydrated Cu-NP sample.

Table 1
Cell parameters and cell volume calculated with the resolved powder patterns applying the Pawley whole-powder pattern decomposition method.

Sample	a [Å]	b [Å]	c [Å]	V [Å^3]	SG	R
Hydrated	7.207195	6.99623	10.38031	1046.89	*Amm2*	0.242
Hydrated	14.41534	6.99627	10.38027	1047.122	*Pnma*	0.193
Dehydrated	7.11529	7.11529	10.93799	533.76	*I4mm*	0.231
Dehydrated	14.83321	12.2363	9.89889	1796.15	*Pnma*	0.139

P and linear in the amount adsorbed adsorption isotherms of carbon dioxide at 273 and 298 K on the Cu-NP sample. This material was pre-activated at 100 °C, a temperature high enough to release all the water present in the micropores as indicated by the TGA data. Meanwhile, to demonstrate that the equilibrium adsorption process is typical of a microporous adsorbent, Fig. 7b shows Dubinin–Radushkevitch (D–R) plots. Since, an immense amount of experimental data indicates that the adsorption process in the micropore range is very well described by the Dubinin–Radushkevitch (D–R) adsorption isotherm equation [17,18]. The Dubinin–Radushkevitch (D–R) adsorption isotherm equation can be represented in a log–log scale, as follows: $\ln(n_a) = \ln(N_a) - (RT/E)^2 \ln(P_0/P)^2$, describing the relation between the amount adsorbed, n_a, and the inverse of the relative pressure, i.e., P_0/P; where E is a parameter named the characteristic energy of adsorption and, N_a is the maximum amount adsorbed in the micropore volume.

It is necessary to state now that the equilibrium adsorption process of vapors in complex porous systems takes place approximately as follows [17,18]: first, micropore filling, where the adsorption behavior is dominated nearly completely by the interactions of the adsorbate, and the pore wall; after that, at higher pressures, external surface coverage, consisting of monolayer, and multilayer adsorption on the walls of mesopores, and open macropores, and finally capillary condensation in the mesopores. We are working in the micropore filling pressure range, $0.0008 < P/P_0 < 0.02$, then we are far from surface coverage, that normally takes place in the $0.05 < P/P_0 < 0.4$ range, and farther from capillary condensation that is the cause of adsorption hysteresis. Consequently, our isotherm is completely reversible, thereafter, we do not need to get the desorption isotherm.

The isotherms (Fig. 7a) were also employed for the calculation of the isosteric heat of adsorption, q_{iso}, using the Clausius–Clapeyron equation:

$$q_{iso} = RT^2 \left[\frac{d\ln P}{dT}\right]_{\Gamma} \approx RT^2 \left[\frac{d\ln P}{dT}\right]_{n_a} \approx RT_1T_2 \left(\frac{\ln P_2 - \ln P_1}{T_2 - T_1}\right)_{n_a} \quad (1)$$

where $\Gamma = n_{ad}/n_{Ab}$ is the ratio of the number of moles of the adsorbate, n_{ad}, and the adsorbent n_{Ad} in the system adsorbate–adsorbent for a microporous material [18,19,36], n_a is the amount adsorbed in mmol/g, T_i is the temperature, and P_i the equilibrium adsorbate pressure at constant loading.

Results of the calculations made with Eq. "(1)" are reported in Fig. 8.

From these results it is possible to conclude that, q_{iso} is nearly constant with respect to the variation of the amount adsorbed, n_a. The mean and standard deviation of the values of q_{iso} reported in Fig. 8 are 30 ± 3 kJ/mol. This fact requires an explanation. During adsorption in micropores, as was previously stated, the adsorption behavior is initially, at very low relative pressure, dominated almost entirely by the interactions of the adsorbate and the pore wall, afterward, at higher pressures, lateral interactions between adsorbate molecules are also present [17]. The process of adsorption is normally energetically heterogeneous as long as the adsorption field inside the micropore is heterogeneous and depends upon the position of the adsorbate inside the adsorption space. That is, the isoteric heat of adsorption should be a decreasing function of the micropore volume recovery, $\theta = n_a/N_m$ [18].

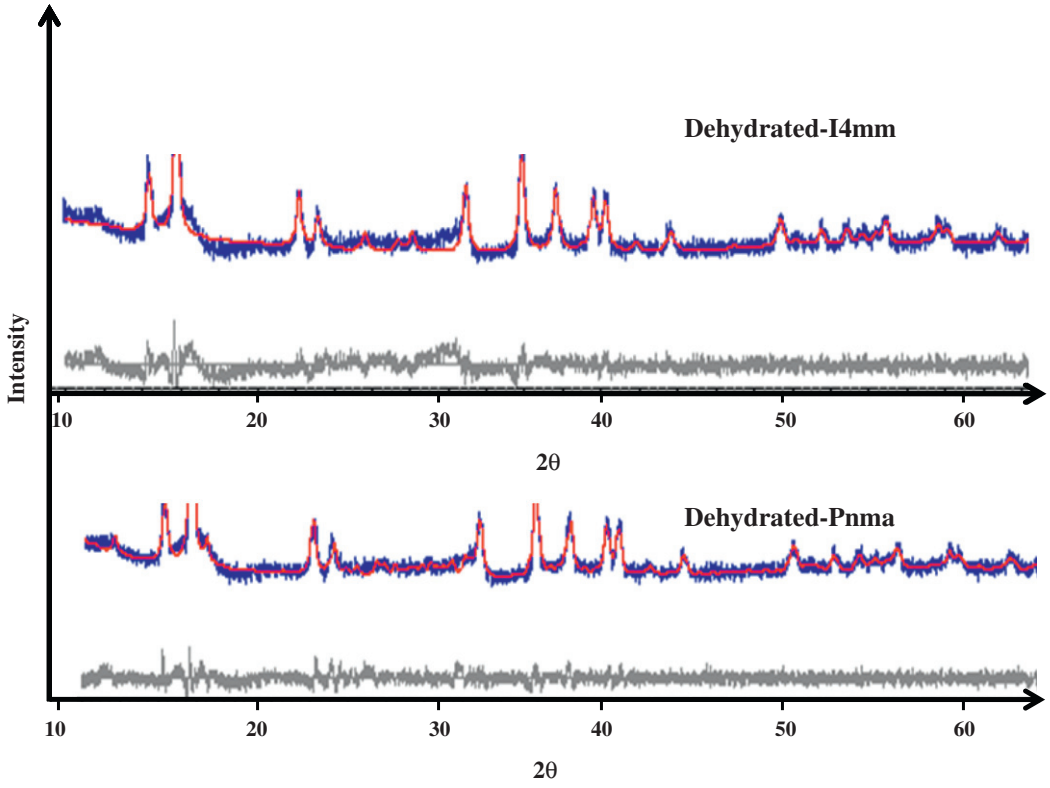

Fig. 6. Pawley refinements of the XRD profile of the dehydrated Cu-NP sample.

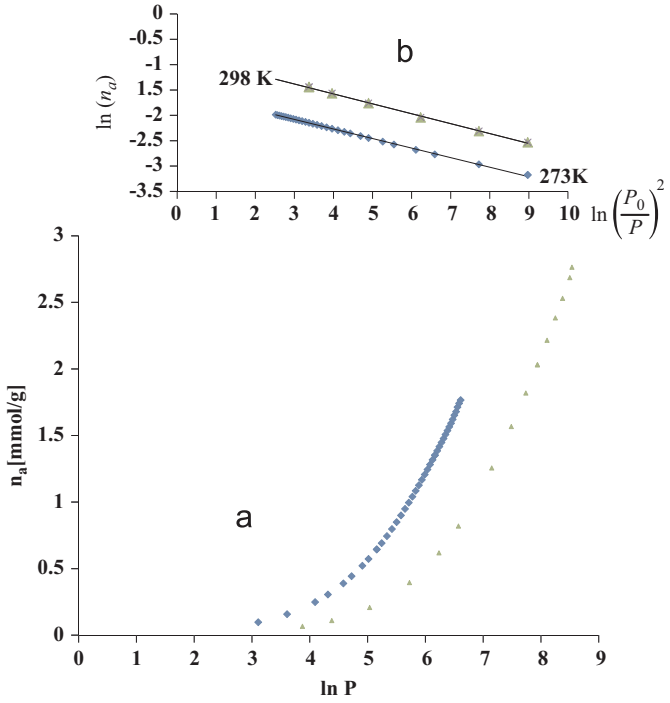

Fig. 7. CO_2 adsorption isotherms in the Cu-NP sample at 273 and 298 K. Semi-logarithmic plot (a), Dubinin–Radushkevitch (D–R) plot (b).

However, in some cases the energetically heterogeneous character of the process is masked by the presence of lateral interactions, which provoke the homogeneization of the adsorption field. That is the adsorption energy corresponding to wall and lateral interactions are mutually compensated to produce, an apparently, homogeneous adsorption energy.

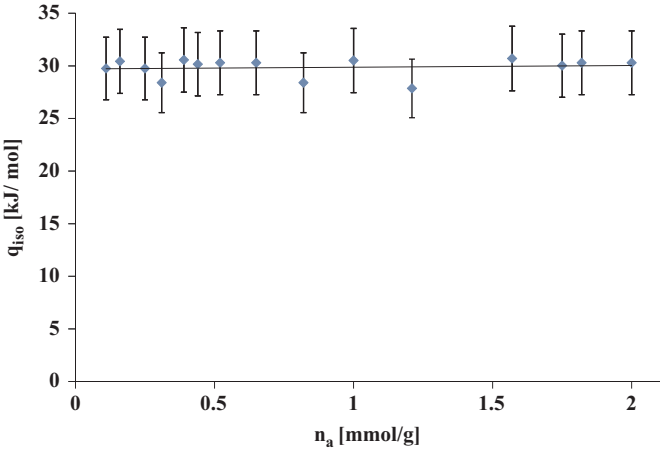

Fig. 8. Isosteric heat of adsorption versus amount adsorbed profile, corresponding to the Cu-NP sample.

The number reported for the isosteric heat of adsorption corresponds to a relatively high amount of adsorption energy. It compares well with values reported for silicalite, a 10MR molecular sieve showing the MFI framework type. To be precise the experimental isosteric heat of adsorption measured for the adsorption of carbon dioxide on silicalite at 296–306 K, in the range: $0.1 < n_a < 1.5$ mmol/g, yields an average a value for q_{iso} of 28 kJ/mol [37]. In addition, for a set of different amorphous silica materials, the isosteric heat of adsorption measured for the adsorption of carbon dioxide at 297 K in the micropore region produces values for q_{iso} around 28 kJ/mol [20]. Similarly, the isosteric heat of adsorption for the adsorption of carbon dioxide at 297 K on Na-SAPO-34 molecular sieve yielded similar values for q_{iso} [38]. It is a very well known fact that the interaction between an adsorbent and a molecule like carbon dioxide, that show a

noticeable quadrupolar moment, $Q_{CO_2} = -4.3 \times 10\text{-}42\,C\,m^2$ [39], comprises a combination of dispersive and electrostatic attractive interactions [20]. It is widely accepted that carbon dioxide interact with microporous frameworks through dispersion and quadrupole interactions [20,37,38,40]. In the case of interest here this is the case as will be below further discussed.

Statistical Physics [17] and the Dubinin theory of volume filling [41] are usually applied to mathematically model the equilibrium adsorption process in microporous crystalline materials; such as: zeolites, metal organic frameworks (MOFs) and other porous coordination polymers, as nitroprussides and then deduce an isotherm equations [17–19,42,43]. To develop the model of interest here [19,42,43], the adsorption space was considered energetically homogeneous and the adsorption process was considered as a 3-D volumetric occupation of the adsorption space [41] and not as a 2-D surface covering process such as the one described by traditional Langmuir processes. The isotherm equation for immobile and mobile adsorption with lateral interactions deduced by means of the Grand Canonical Ensemble [17], following the conditions previously imposed, has the following form [19,42]:

$$\theta = \frac{n_a}{N_a} = \frac{KP}{1+KP} \tag{2}$$

$$K_l = K_0 \exp\left(\frac{[(E_0^g - E_0^a)]}{RT}\right)\exp\left(\frac{k\theta}{RT}\right) \tag{3}$$

where K_0 is a constant for $T=const$, different for the mobile and immobile cases, E_0^g is the reference energy state for the gas molecule, E_0^a is the reference energy state for the adsorbed molecule in the homogeneous adsorption field inside the cavity or channel, k is a constant characterizing the lateral interactions, and $\theta = n_a/N_a$, where, n_a is the amount adsorbed and, N_a is the maximum amount adsorbed in the volume of the micropore. Eq. (2) is a Fowler–Guggenheim Type (FGT) adsorption isotherm equation; but, describing a volume filling rather than a surface coverage. For $k=0$ Eq. (2) reduces to a Langmuir Type (LT) adsorption isotherm equation, but still well describing a volume filling instead of a surface coverage. Then, for $k \approx 0$, we can plot the LT equation:

$$n_a = \frac{N_a KP}{1+KP} \tag{4}$$

where K is a constant for $T=const$, that could be estimated with the help of a least square non-linear fitting process. The fitting process was carried out with the peak separation and analysis software PeakFit (Seasolve Software Inc., Framingham, Massachusetts) based on the least square procedure [44], and the results are gathered in Table 2. This method allowed for reliable measurement of the micropore volume ($W_{MP} = N_a V_L$; in which, $V_L = 41.3\ cm^3/g$ is the molar volume CO_2 at 273 K) for the studied polymorph.

The FGT isotherm equation type can be also written as follows:

$$\ln\left(\frac{\theta}{1-\theta}\right) = \ln K + \frac{k\theta}{RT} \tag{5}$$

Table 2
Microporous volume calculated by fitting the Langmuir-type (lt) isotherm for volume filling in a microporous adsorbent in linear form to the obtained adsorption data.

Sample	T [K]	R^2	$W_{MP}^{CO_2}$ [cm^3/g]	K [g Torr/mmol]
Cu-NP	273	0.9999	0.154	0.00119590
Cu-NP	298	0.9996	0.185	0.00030256

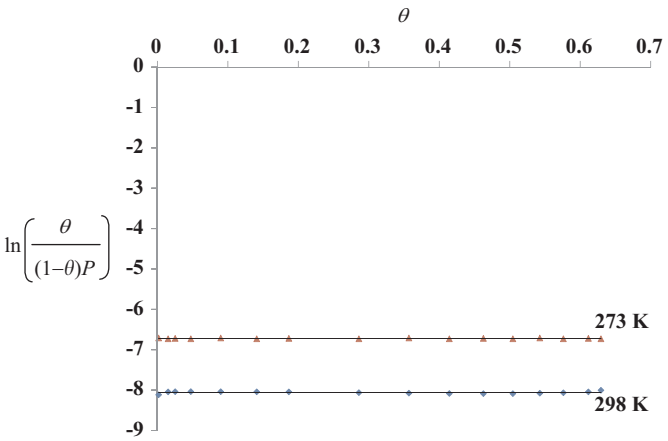

Fig. 9. FGT plots for the adsorption of CO_2 on the Cu-NP sample 273 and 298 K.

Table 3
Parameters calculated by fitting the Fowler–Guggenheim Type (FGT) isotherm in linear form to the obtained adsorption data.

Sample	T [K]	k	ln$K$	q_{iso} [kJ/mol]
Cu-NP	273	0.0049	−6.721	36 ± 3
Cu-NP	298	0.0056	−8.058	36 ± 3

A fit of this isotherm is shown in Fig. 9 and the parameters are gathered in Table 3. This plot experimentally establishes that $k \approx 0$. Therefore, it is our assessment that the analysis of the adsorption data with the help of the LT type adsorption isotherm for volume filling is very accurate.

Now, with the values calculated for K, at two different temperatures (Tables 2 and 3) and the following expression is obtained [29]:

$$K = K_0 e^{q_{iso}(0)/RT} \tag{6}$$

We can estimate the isosteric heat of adsorption for zero loading $q_{iso}(0)$. The obtained value $q_{iso}(0) = 36 \pm 3$ kJ/mol is close to the average value measured with the help of the isosteric method. It is necessary state now that the values of K calculated by plotting Eqs. (6) (Table 2) and (7) (Table 3) are equivalent within the experimental error. This fact indicates the consistency within the obtained data.

The micropore volume data (Table 2) evidence an increase in the micropore volume with increasing temperature from $W_{MP}^{CO_2} = 0.153\,cm^3/g$ at 273 K to $W_{MP}^{CO_2} = 0.181\,cm^3/g$ at 298 K. This fact explains the large amount of adsorption of carbon dioxide at 298 K and 6.7 atm. measured ($n_a = 0.122$ g/g, that is: 12.2 Wt%). Since, the framework of the orthorrhombic *Pnma* polymorph resembles a stack of rippled sheets interconnected by cyanide bonds [8], it is possible to assume that the distance between sheets increases with temperature causing the observed increase in the micropore volume with rising temperature.

The pore size of the orthorhombic framework of the tested nitroprusside is close to the kinetic diameter of the carbon dioxide molecule. This fact causes an effect named confinement [45–47] or surface interaction potential overlapping that favors relatively strong dispersion and repulsion interactions between the framework of the adsorbent and the adsorbed molecule. This force, combined with the interaction between the quadrupole moment of the carbon dioxide molecule and the nitroprusside framework electric field gradient, which is as well enhanced by the confinement, are the major contributions to the adsorption energy. Then, the confinement effect justifies the relatively high

value measured for the adsorption energy in a physical adsorption process that binds the carbon dioxide molecule inside the nitroprusside micropores, by the influence of the dispersive forces and the attraction of the quadrupole interaction [20]. Calculations made with the help of the Horvath–Kawazoe method and applying the Saito–Foley equations [17,18] for cylindrical pores in silica have shown that these forces; specifically, London forces and quadrupole interactions, contributes about 90% of the whole interaction [20].

To get information about further contributions to the interaction between the nitroprusside framework and the carbon dioxide molecule further DRIFTS studies were made. In this regard, a DRIFTS spectrum of carbon dioxide adsorbed on the tested polymorph at 300 K was obtained.

The resolved carbon dioxide IR spectrum (deconvoluted by fitting three Lorentz functions with the help of a least square procedure [44]) and the corresponding data are reported in Fig. 10 and Table 4, respectively. This spectrum shows that the carbon dioxide molecule has some direct interactions with the nitroprusside framework; as evidenced by the presence of three peaks in the observed experimental absorption band. The free carbon dioxide molecule belongs to the $D_{\infty h}$ point group symmetry, showing four fundamental vibration modes, that is, the symmetric stretching, ν_1 (1338 cm^{-1}) the doubly degenerate bending vibration, ν_{2a} and ν_{2b} (667 cm^{-1}), and the asymmetric stretching vibration ν_3 (2349 cm^{-1}) [21–23].

The ν_2 and ν_3 modes are infrared active, whereas ν_1 is only Raman active, in the free molecule [23]. However, when a carbon dioxide molecule interacts with a surface it is no longer a free molecule, and its symmetry is lowered. As a result the ν_1 mode becomes infrared active, and a small band is observed [22], whereas the other modes undergo moderate changes in wave number [23].

The asymmetric stretching vibration, ν_3, of the adsorbed carbon dioxide molecule was observed at 2338 cm^{-1} (Fig. 10).

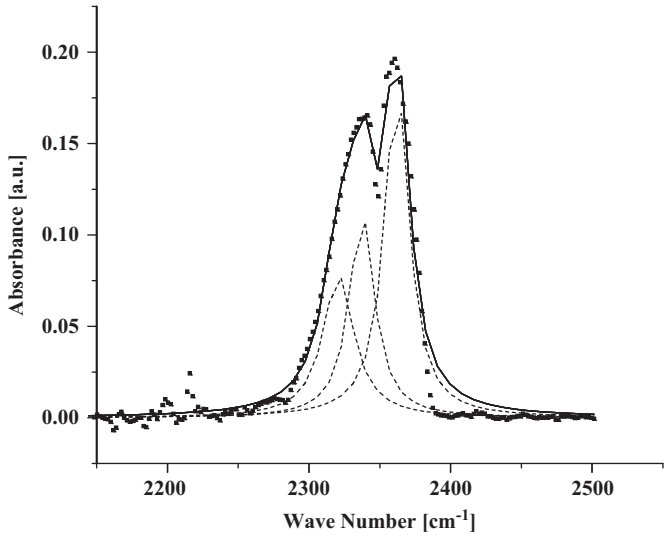

Fig. 10. DRIFTS spectrum CO_2 adsorbed on the Cu-NP sample.

Table 4
Resolved peaks positions of the DRIFTS spectra of carbon dioxide adsorbed on the tested Cu-nitroprusside.

Sample	x_c^1 [cm^{-1}]	A_1 [%]	x_c^2 [cm^{-1}]	A_2 [%]	x_c^3 [cm^{-1}]	A_3 [%]
Cu-NP	2321	0.26	2338	0.28	2362	0.46

This band corresponds to carbon dioxide physically adsorbed [48] onto the nitroprusside framework surface. The smaller band at about 2321 cm^{-1} is normally assigned to a combination band [22], while, the absorption band observed at around 2338 cm^{-1} is the result of the attachment of the carbon dioxide molecule by dispersive and electrostatic forces to the adsorption space defined by the Cu-NP micropores. The adsorption process produces the confinement of the carbon dioxide molecule and thereafter the frequency shift and explains the band observed at 2338 cm^{-1} and the combination band. This state of the carbon dioxide molecule is equivalent to one of zeolitic water.

In addition there is observed another band observed at 2362 cm^{-1} that should correspond to adsorption of carbon dioxide on an electron accepting Lewis acid site [21]. An example of this type of adducts was recently reported [49] in a study of the adsorption of carbon dioxide in the molecular organic framework MIL-100, where a ν_3 band was found at 2351 cm^{-1} and assigned to the following species: $Cr^{3+}.\bullet\bullet\bullet O{=}C{=}O$. In our case the band at 2362 cm^{-1} should characterize the interaction of the carbon dioxide molecule with the Cu^{2+} located in the framework of the Cu-nitroprusside forming following adduct: $Cu^{2+}.\bullet\bullet\bullet O{=}C{=}O$. This state of the carbon dioxide molecule is equivalent to that of coordinated water.

The DRIFTS data indicates the existence of two adsorption states for the carbon dioxide molecule, one of them a state where the molecule interacts with the Cu^{2+} located in the framework of the Cu-NP which acts as an electron accepting Lewis acid site [50]. The Lewis acid–base reaction results in more or less stable adducts, whose steadiness can be effectively explained by the model of the hard and soft acids and bases scheme [51]. That is, an acid–base adduct is produced by the charge transfer from the HOMO of the base to the LUMO of the acid [52].

In our case the importance of this finding is related to the fact that the Cu^{2+} is located in the framework of the Cu-NP in a site accessible to adsorbed molecules. Therefore, it is possible to assume that an acid–base interaction between Cu^{2+} and small basic molecules producing a charge transfer which could be detected for example by a change in the magnetic susceptibility [16] of the nitroprusside. Besides, this Cu^{2+} site is intrinsically a catalytic site [53].

The adsorption of carbon dioxide has been recently studied on a dehydrated Prussian blue analog $Co_3^{II}[Co^{III}(CN)_6]_2$ [54,55] with the help of DRIFTS. It was found an infrared band at 2340 cm^{-1} that was assigned to adsorbed carbon dioxide and reported the following enthalpy of adsorption $\Delta H_{ad} = -23 \pm 3$ kJ/mol [54]. These results are similar to the data reported in the present paper.

4. Summary

A thorough structural characterization of the synthesized Cu-NP was necessary in order to unambiguously identify the studied polymorph among possible variants. TGA and DRIFTS techniques were employed to study the dehydration process in the as-synthesized Cu-NP polymorph. It was shown that such dehydration process is characteristic of the stable orthorrhombic *Pnma* Cu-NP. Fitting the XRD powder profile data via the Pawley method, indicates that the hydrated polymorph, crystallizes in the orthorhombic *Pnma* space high temperature XRD group (a=14.41534 Å, b=6.99627 Å, c=10.38027 Å). Meanwhile, the best fitting for the *in situ* XRD profile of the anhydrous phase indicate that it also crystallizes in the orthorhombic space group *Pnma* (a=14.83321 Å, b=12.23268 Å, c=9.89889 Å).

A carbon dioxide adsorption study was used to calculate the corresponding isosteric heat of adsorption, indicating an average interaction of 30 kJ/mol and nearly independent of loading. This

indicates that the adsorption space of the studied material is apparently energetically homogeneous and the adsorption field is fairly strong within the physisorption range. Furthermore, it appears that the high adsorption interaction energy is the result of the confinement of the carbon dioxide molecule in the nitroprusside framework pores

Applying Statistical Physics methods, particularly the Grand Canonical Ensemble and the Dubinin theory for pore volume filling, allowed us to develop a set of isotherm equations suitable for the quantification of carbon dioxide adsorption onto the tested Cu-NP. The thorough calculations demonstrated that the studied polymorph showcase an increase of the micropore volume with an increase in temperature which correlates with the high adsorption amount observed at 298 K and 6.7 atm.

A DRIFTS study revealed a band at ca. 2338 cm^{-1} probably related to carbon dioxide physically adsorbed carbon dioxide onto the surface of the nitroprusside framework micropores. The state of the carbon dioxide molecule is similar to zeolitic water. In addition a peak observed at 2362 was related to an interaction of carbon dioxide with $Cu2^{+}$ which probably act as an electron accepting Lewis acid site according to the following adduct: Cu^{2+}.•••O=C=O. This state of the carbon dioxide molecule should correlate to that of coordinated water.

In general this study indicates that the studied polymorph should be considered a suitable adsorbent material for gases due to the available micropore volume and adsorption interaction within the adsorption space. It is hypothesized that upon dehydration small guest molecules could interact with Cu^{2+} and change its magnetic properties resulting this in a potential platform for the development of gas sensors.

Acknowledgments

The authors R.R.M., C.L., R.P., F.M. and F.L. acknowledge the financial support provided by the US Department of Energy through the Massey Chair project at the University of Turabo and recognize the support of the National Science Foundation under the project CHE-0959334. We as well appreciate the collaboration of Bruker AXS Inc. in the training of our personnel in the operation of the D8 Advance System. Finally, we express our gratitude to Teresita Navedo, Geidy Garcia and Dr. Jose Duconge for its help during the characterization process and to Dr. Wilfredo Otaño for allowing us the use of the SEM-EDAX facilities of the University of Puerto Rico, Cayey Campus.

References

[1] H.J. Buser, D. Schwarzenbach, W. Petter, A. Ludi, Inorg. Chem. 16 (1977) 2704.
[2] S.S. Kaye, H.J. Choi, J.R. Long, J. Am. Chem. Soc. 130 (2008) 16921.
[3] D.A. Pejakovic, J.L. Manson, J.S. Miller, A. Epstein, J. Phys. Rev. Lett. 85 (2000) (1994) 2000.
[4] S.S.R. Kaye, J.R. Long, J. Am. Chem. Soc. 127 (2005) 6506.
[5] P.T. Manoharam, W.C. Hamilton, Inorg. Chem. 2 (1963) 1043.
[6] D.F. Mullica, E.L. Sappenfield, D.B. Tippin, D.H. Leschnitzer, Inorg. Chim. Acta 164 (1989) 99.
[7] D.F. Mullica, D.B. Tippin, E.L. Sappenfield, J. Coord. Chem. 24 (1991) 83.
[8] D.F. Mullica, D.B. Tippin, E.L. Sappenfield, J. Coord. Chem. 25 (1992) 175.
[9] E. Reguera, A. Dago, A. Gomez, J.F. Bertran, Polyhedron 15 (1996) 3139.
[10] K.E. Funck, M.G. Hilfiger, C.P. Berlinguette, M. Shatruk, W. Wernsdorfer, K.R. Dunbar, Inorg. Chem. 48 (2009) 3438.
[11] A. Gomez, E. Reguera, L.M.D. Cranswick, Polyhedron 20 (2001) 165.
[12] G. Boxhoorn, J. Moolhuysen, J.P.G. Coolegem, R.A. van Santen, J. Chem. Soc., Chem. Commun. (1985) 1305.
[13] J. Balmaseda, E. Reguera, A. Gomez, J. Roque, C. Vazquez, M. Autie, J. Phys. Chem. B 107 (2003) 11360.
[14] J.T. Culp, C. Matranga, M. Smith, E.W. Bittner, B. Bockrath, J. Phys. Chem. B 110 (2006) 8325.
[15] L. Reguera, J. Balmaseda, C.P. Krap, E. Reguera, J. Phys. Chem. C 112 (2008) 10490.
[16] M. Zentková, M. Mihalik, I. Tóth, Z. Mitróová, A. Zentko, M. Sendek, J. Kovác, M.M. Lukácová, M. Marysko, M. Miglierini, J. Magn. Magn. Mat. 272–276 (2004) E753.
[17] R. Roque-Malherbe, Adsorption and Diffusion in Nanoporous Materials, CRC Press, Boca Raton, Florida, 2007.
[18] R. Roque-Malherbe, The Physical Chemistry of Materials: Energy and Environmental Applications, CRC Press, Boca Raton, Florida, 2009.
[19] R. Roque-Malherbe, Mic. Mes. Mater. 41 (2000) 227.
[20] R. Roque-Malherbe, R. Polanco-Estrella, F. Marquez-Linares, J. Phys. Chem. C 114 (2010) 17773.
[21] J.C. Lavalley, Catal. Today 27 (1996) 377.
[22] A.L. Goodman, L.M. Campus, K.T. Schroeder, Energy Fuels 19 (2005) 471.
[23] F.X. Llabres i Xamena, A. Zecchina, Phys. Chem. Chem. Phys. 4 (2002) 1978.
[24] D. Cazorla-Amoros, J. Alcañiz-Monge, M.A. de la Casa-Lill, A. Linares-Solano, Langmuir 14 (1998) 4589.
[25] Quantachrome Instruments, Powder Tech Note 35.
[26] J.A. Dunne, M. Rao, S. Sircar, R.J. Gorte, A.L. Myers, Langmuir 12 (1996) 5896.
[27] Z. Bacsik, R. Atluri, A.E. Garcia-Bennett, N. Hedin, Langmuir 26 (2004) 10013.
[28] M. Kurmoo, Chem. Soc. Rev. 38 (2009) 1353.
[29] K. Nakamoto, Infrared and Raman Spectra of Inorganic and Coordination Compounds: Part A: Theory and Applications in Inorganic Chemistry, J. Wiley and Sons, New York, 1997.
[30] M. Holzbecher, O. Knop, M. Falk, Canadian J. Chem. 49 (1971) 1413.
[31] A. Benavente, J.A. de Moran, O.E. Piro, E.E. Castellano, P.J. Aymonino, J. Chem., Crystallography 27 (1997) 343.
[32] P.J. Aymonino, Pure Appl. Chem. 60 (1988) 1257.
[33] H. Toraya, Rigaku J. 6 (1989) 28.
[34] G.S. Pawley, J. Appl. Cryst. 14 (1984) 357.
[35] H. Omi, T. Ueda, K. Miyakubo, T. Eguchi, App. Surf. Sci. 252 (2005) 660.
[36] R. Roque-Malherbe, J. Thermal Anal. 32 (1987) 1361.
[37] J.A. Dunne, R. Mariwala, M. Rao, S. Sircar, R.J. Gorte, A.L. Myers, Langmuir 12 (1996) 5888.
[38] A.G. Arévalo-Hidalgo, J.A. Santana, R. Fu, Y. Ishikawa, A.J. Hernández-Maldonado, Mic. Mes. Mater. 130 (2010) 142.
[39] A.D. Buckingham, Proc. R. Soc. Ser. A 273 (1963) 275.
[40] R. Bai, J. Deng, R.T. Yang, Langmir 19 (2003) 2776.
[41] B.P. Bering, M.M. Dubinin, V.V. Serpinskii, J. Colloid Interface Sci. 38 (1972) 185.
[42] R. Roque-Malherbe, KINAM 6 (1984) 135.
[43] C. de la Cruz, C. Rodriguez, R. Roque-Malherbe, Surf. Sci. 209 (1989) 215.
[44] N.R. Draper, Smith, Applied Regression Analysis, 3rd Ed., John Wiley & Sons, New York, 1998.
[45] E.G. Derouane, Zeolites Micropoorous Solids: Synthesis, in: E.G. Derouane, F. Lemos, C. Naccache, F. Ramos-Riveiro (Eds.), Structure and Reactivity, Kluwer Academic Publishers, Dordrecht, 1992, p. 511.
[46] L. Yang, K. Trafford, O. Kresnawahjuesa, J. Sÿepa, R.J. Gorte, D. White, J. Phys. Chem. B 105 (2001) 1935.
[47] R. Roque-Malherbe, F. Diaz-Castro, J. Mol. Catal. A 280 (2008) 194.
[48] A.L. Goodman, Energy Fuels 23 (2009) 1101.
[49] P.L. Llewellyn, S. Bourrelly, C. Serre, A. Vimont, M. Daturi, L. Hamon, G. De Weireld, J.-S. Chang, D.-Y. Hong, Y.K. Hwang, S.H. Jhung, G. Ferey, Langmuir 24 (2008) 7245.
[50] H. Knozinger, S. Huber, J. Chem. Soc., Faraday Trans. 94 (1998) 2047.
[51] R.G. Pearson, Chemical Hardness: Applications from Molecules to Solids, Wiley-VCH, Weinheim, 1997.
[52] S. Mebs, S. Grabowsky, D. Forster, R. Kickbusch, M. Hartl, L.L. Daemen, W. Morgenroth, P. Luger, B. Paulus, D. Lentz, J. Phys. Chem. A 114 (2010) 10185.
[53] A. Corma, H. Garcıa, Chem. Rev. 103 (2002) 4307.
[54] C.F. Windisch, P.K. Thallapally, B.P. McGrail, Spectrochim. Acta, Part A 74A (2009) 629.
[55] C.F. Windisch, P.K. Thallapally, B.P. McGrail, Spectrochim. Acta, Part A 77A (2010) 287.